

## RESEARCH PAPER

# Theoretical Study of The Reaction of Ketene with Methanimine Using DFT Method

Haydar A. Mohammad-Salim

Department of Chemistry, Faculty of Science, University of Zakho, Duhok 42001, Kurdistan Region, Iraq

### ABSTRACT:

The Density Functional Theory (DFT) method was used to investigate the stepwise mechanism of the [2+2] cycloaddition (22CA) reaction of ketene with methanimine at the B3LYP/6-311++G(d,p) level of theory. Two modes of attack between reactants were investigated, yielding Azetidin-2-one from *path1* and Azetidin-2-one from *path2* as two possible products passing through two different transition states. The geometry of transition states and products was analysed. The study of stationary points and energetic parameters shows that the reaction mechanism is stepwise and that Azetidin-2-one **P1** is thermodynamically and kinetically more favoured than Azetidin-3-one **P2**. The analysis of the frontier molecular HOMO and LUMO orbitals shows that the Azetidin-2-one **P1** is more stable due to its higher energy gap. The global electronic flux from the strong nucleophilic ketene **R1** to the methanimine **R2** is predicted using conceptual density functional theory (CDFT) indices. Reactant's electrophilic and nucleophilic Fukui functions were also investigated.

KEY WORDS: *Stepwise mechanism; [2+2] cycloaddition; DFT; CDFT; Fukui Functions.*

DOI: <http://dx.doi.org/10.21271/ZJPAS.33.4.1>

ZJPAS (2021), 33(4); 1-10 .

### 1.INTRODUCTION :

The chemistry of heterocycles has advanced dramatically in recent years, and This family of molecules is the basis for the majority of compounds produced in the fields of industrial pharmaceutical chemistry (King et al., 2019; H. A. Mohammad-Salim & Abdallah, 2019b; Sowmya, Lakshmi Teja, Padmaja, Kamala Prasad, & Padmavathi, 2018). It's worth noting that heterocycles make up two-thirds of all compounds mentioned in the literature (Barber et al., 2018; Glasnov, 2018; Pawlowski, Stanek, & Stodulski, 2019). Therefore, it's understandable that heterocyclic compounds have become the focus of interest of a wide group of experimental and theoretical chemists.

One of the most effective synthetic strategies that requires the formation of different membered rings is cycloaddition reactions. These reactions occur when two unsaturated reactants interact. Among cycloaddition reactions, the 22CA reaction is one of the reactions used to build the four-membered ring and it is a structural unit in pharmaceutical compounds and natural occurring products (H. A. Mohammad-Salim & Abdallah, 2019a; H. A. Mohammad-Salim, Abdallah, Maiyelvaganan, Prakash, & Hochlaf, 2020; H. A. M. Salim, H. H. Abdallah, & P. Ramasami, 2018). The hetero-22CA reactions have been given attention by researchers due to their wide applications in the synthesis organic chemistry (Flores & Schmidt, 2019; Pang et al., 2018; H. M. Salim, H. H. Abdallah, & P. Ramasami, 2018). The four-membered heterocycles are the heterocyclic analogues of cyclobutane and are considered to be derived from cyclobutane by replacing a methylene group (-CH<sub>2</sub>) with a heteroatom, usually, oxygen, sulfur or nitrogen.

#### \* Corresponding Author:

Haydar Mohammad-Salim  
E-mail: hayder.salim@uoz.edu.krd

#### Article History:

Received: 20/03/2021

Accepted: 22/04/2021

Published: 18/08 /2021

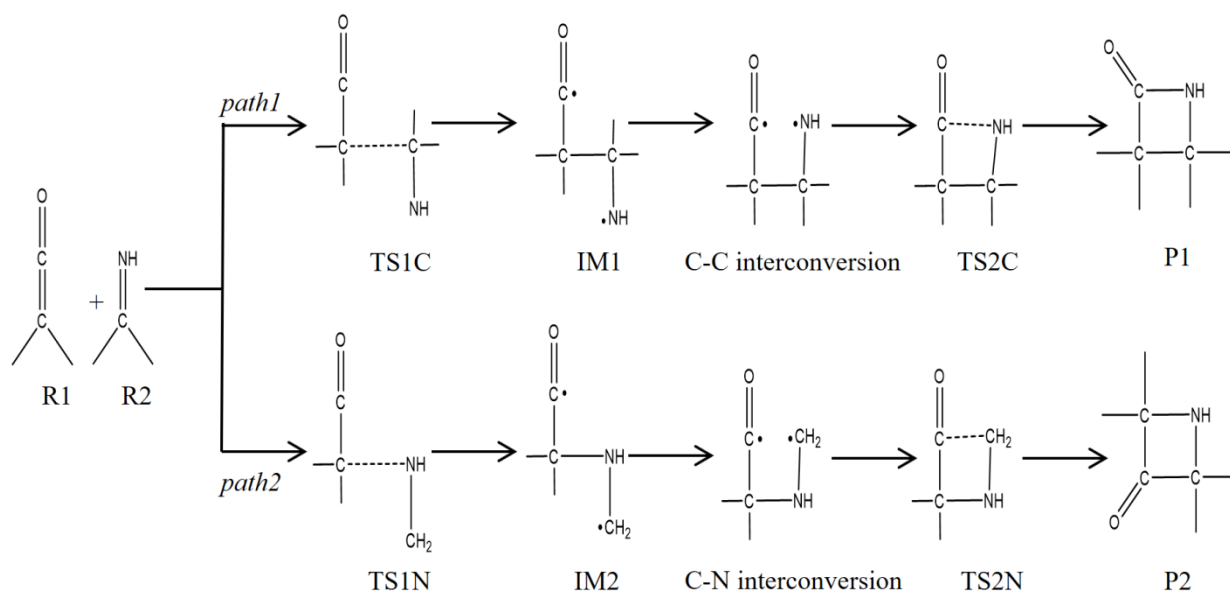
The saturated heterocycles of four-membered containing oxygen, sulfur and nitrogen are called oxetane, thietane and azetidine, respectively. The small heterocycles with two heteroatoms, e.g. oxaphosphetanes and thioanalogues prepared from Wittig reaction intermediate, also attract researchers due to their reactivity (Espinosa Ferao & Streubel, 2020; A. Kyri *et al.*, 2018; A. W. Kyri *et al.*, 2019).

In the previous two decades, computational chemistry has been an effective method for analyzing experimentally observed selectivity and reactivity results by creating a formal description of chemical reaction mechanisms (Krylov *et al.*, 2018). Despite the a number of modern uses of computational science in chemistry, the underlying theories of organic chemistry, since last 40 years. had not experienced major breakthrough, Domingo suggested the molecular electron density theory in 2016 to acknowledge the crucial role of electron density variations in molecular reactivity (Domingo, 2016; Ríos-Gutiérrez & Domingo, 2019). This theory has been successfully analyzing the experimental results of many cycloaddition reactions for the past four years (Domingo, Ríos-Gutiérrez, & Pérez, 2018; H. Mohammad-Salim, Hassan, Abdallah, & Oftadeh, 2020; H. A. Mohammad-Salim; H. A. Mohammad-Salim, Acharjee, & Abdallah, 2021; H. A. Mohammad-Salim,

Basheer, Abdallah, Zeroual, & Jamil, 2021; Ríos-Gutiérrez & Domingo, 2019). Recently, this theory has been applied to analyse the experimental outcome of strain promoted and catalysed cycloaddition reactions and the observed chemo-, stereo- and regioselective synthesis of heterocyclic compounds (Abbiche *et al.*, 2020; Acharjee, Mohammad-Salim, Chakraborty, Rao, & Ganesh; Domingo, Acharjee, & Mohammad-Salim, 2020; H. A. Mohammad-Salim, Acharjee, Domingo, & Abdallah, 2020).

Since four-membered heterocycles have industrial uses such as potential drugs, catalysts and dye-sensitized solar cells (Fuentes de Arriba, Lenci, Sonawane, Formery, & Dixon, 2017; Mathew *et al.*, 2014; Xu, Zhang, & Luo, 2014), the analysis of these compounds is of considerable interest. Preparation of nitrogen containing heterocyclic compounds have become a major point of interest among researchers due to its biological activities and success in the involvement of cancer treatment (Tokunova *et al.*, 2001; Willenbring & Tantillo, 2008). Therefore, the primary goal of this investigation was to study the stepwise mechanism path of 22CA of ketene **R1** with methanimine **R2** (see Scheme 1) using theoretical methods in more details.

**Scheme 1.** Mechanism of the 22CA reaction between ketene (**R1**) and methanimine (**R2**).



## 2.COMPUTATIONAL METHODS

The Gaussian 16 package was used to do all calculations under the Linux operating system (Frisch *et al.*, 2009). The B3LYP functional in DFT method has been shown to be a suitable method for studying 22CA reactions and is used in this study (R.G. Parr & Weitao, 1989; Saha *et al.*, 2019; Svatunek, Pemberton, Mackey, Liu, & Houk, 2020). Throughout, B3LYP functional is used in conjunction with the 6-311++G(d,p) basis set (Ditchfield, Hehre, & Pople, 1971; Lee, Yang, & Parr, 1988). Geometry optimization on geometry convergence, electron density (SCF) convergence and integration grid were carried out in default settings.

The existence of one imaginary frequency was confirmed by frequency measurements at the optimized TSs, while in the case of the local minimum, the absence of imaginary frequency was confirmed. Intrinsic Reaction coordinate (IRC) calculations were performed using the Gonzales–Schlegel integration approach to validate the minimum energy reaction pathway linking the reactants and products through the defined TSs (Fukui, 1970; Gonzalez & Schlegel, 1991). The CDFT indices are computed using the equation discussed by Parr and co-workers (Robert G. Parr & Pearson, 1983; R.G. Parr & Weitao, 1994).

The electrophilic  $f_k^+$  and nucleophilic  $f_k^-$  Fukui functions (Domingo, Pérez, & Sáez, 2013), which allow for the description of the nucleophilic and electrophilic centers of a reactants, were calculated via the examination of the Mulliken atomic spin density of the radical anion and the radical cation of ketene **R1** and methanimine **R2**, from the optimized neutral geometries, using single-point energy calculations.

## 3.RESULTS AND DISCUSSION

Two regioisomeric paths, namely the *path1* and *path2* (see Scheme 1), for these 22CA reactions are feasible, due to non-symmetry of the reactants. The *path1* reaction path is related with the formation of Azetidin-2-one (**P1**), while the *path2* channel with the formation of Azetidin-3-one (**P2**), passing through different transition states.

The electronic energy profile for the 22CA reaction of **R1** with **R2** is shown in Figure 1. This figure shows the all possible transition states and intermediates associate with the reaction of ketene **R1** with methanimine **R2**. The electronic energies (in kcal/mol) are relative to the energy of the two non-interacting reactants. Similarly, the relative energy for **P2** is about 22 kcal/mol above the energy of **P1**. It's worth to realize that the product **P1** is a kinetic as well as thermodynamic product. It can be noted that there are two pathways of this reaction. One of them is to obtain **IM1** intermediate passing through **TS1C** and the other is to form **IM2** intermediate passing through **TS1N**. The results of electronic energy prefer the first pathway over the other. The electronic energy of **IM2** intermediate is slightly above the most stable **IM1** intermediate.

The **IM1** and **IM2** diradical intermediates are formed via **TS1C** and **TS1N** transition states, respectively. The activation energy is higher for the **TS1N** transition structure than the transition structure **TS1C**. Therefore, the *path1* for obtaining **P1** is expected to be the rate determining step. The next step of this reaction path corresponds to a rotation of the C-C and C-N bonds through the transition states **TS2C** and **TS2N** to form the product **P1** and **P2**, respectively. The activation energy of this step is around 21 kcal/mol for **TS2C** and 30 kcal/mol for **TS2N**, respectively, such activation energies are obviously typical for the internal rotation of C-C and C-N single bond.

Table 1 lists the thermodynamic parameters for the 22CA reactions of **R1** with **R2** obtained in the gas phase with B3LYP/6-311++G(d,p) method. The first activation enthalpy for **TS1C** is 59.98 kcal/mol and for **TS1N** is 62.95 kcal/mol, while the second activation enthalpy for **TS2C** 61.89 kcal/mol while for **TS2N** is 67.85 kcal/mol. The values of Gibbs free energy for **P1** is -14.60 kcal/mol, which refers to the spontaneous reaction. However, the Gibbs free energy for **P2** is 7.61 kcal/mol that refers to the non-spontaneous reaction. The enthalpy of azetidin-2-one **P1** azetidin-3-one **P2** is negative, indicating the stability of both products. The observed data of thermodynamic parameters can be used to reach the conclusion that the product **P1** is formed faster and has negative Gibbs free energy, thus **P1** is preferred kinetically as well as thermodynamically.

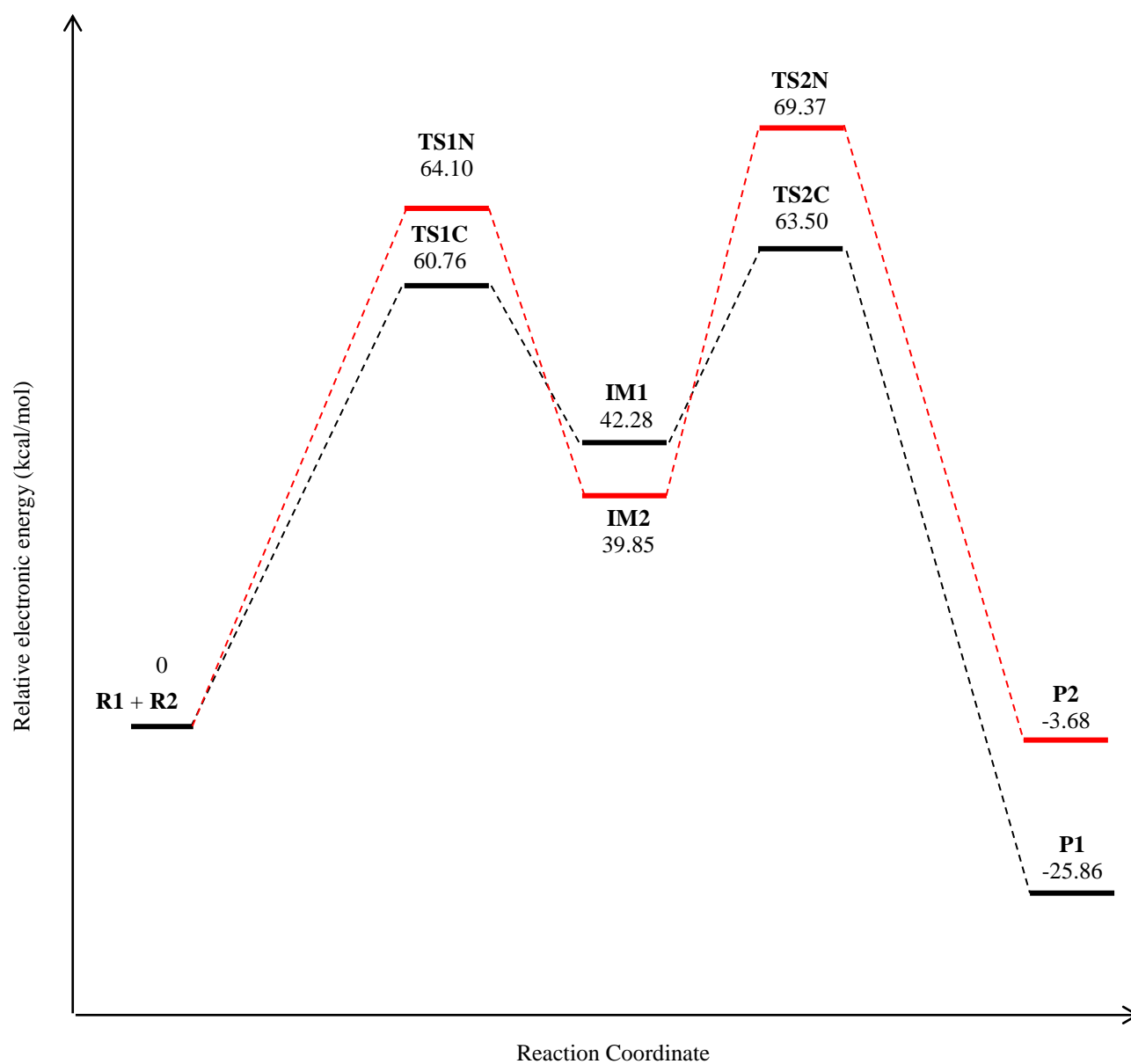


**Figure 1.** Relative electronic energies ( $\Delta G$ ) in kcal/mol of stationary points associated with the 22CA reaction of ketene with methanimine.

**Table 1.** Thermodynamic parameters for transition states, intermediates and products at B3LYP/6-311++G(d,p) level of theory in (kcal/mole) for  $\Delta H$  and  $\Delta G$  and in (cal/mol.K) for  $\Delta S$ .

Species	$\Delta H$	$\Delta G$
TS1C	59.98	69.91
IM1	41.55	51.56

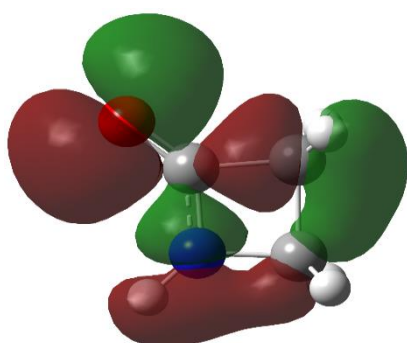
<b>TS2C</b>	61.89	73.94
<b>P1</b>	-27.53	-14.60
<b>TS1N</b>	62.95	74.67
<b>IM2</b>	39.45	48.41
<b>TS2N</b>	67.85	79.64
<b>P2</b>	-5.39	7.61

Table 2 lists the HOMO and LUMO energies in eV computed at the B3LYP level of theory for reactants and products. As shown from the results in the table, the energy gap for **R1** is lower than

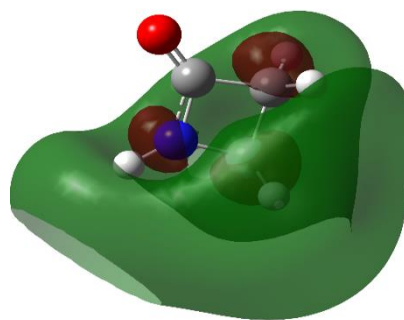
the energy gap for **R2**. It is worth to realize that the product **P1** has a wider energy gap than the product **P2**, indicating the stability of this product.

**Table 2.** HOMO energies, LUMO energies and energy gap (in eV unit) for reactants and products at B3LYP/6-311++G(d,p) level of theory.

eV	HOMO	LUMO	Energy Gap
<b>R1</b>	-7.20	-0.82	5.61
<b>R2</b>	-6.86	-1.75	6.69
<b>P1</b>	-6.70	-1.54	6.84
<b>P2</b>	-6.83	-1.75	5.73

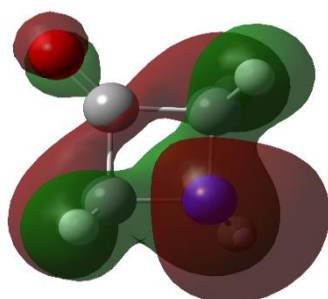


**HOMO**

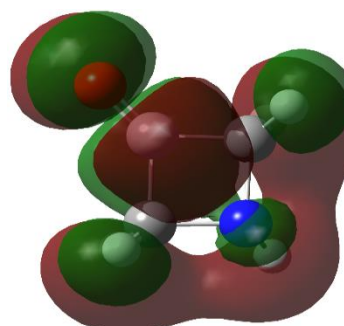


**LUMO**

**P1**



**HOMO**



**LUMO**

**P2**

**Figure 2.** The HOMO and LUMO of the **P1** and **P2** cycloadducts at B3LYP/6-311++G(d) level of theory.

Their energies are given in Table 2.

The optimized geometries of all transition states at B3LYP/6-311++G(d,p) method are shown in Figure 3. The distances between C1 and C3, and C1 and N4 interacting centers at the transition states are: 2.15 Å at **TS1C** and 1.76 Å at **TS1N**. However, for the second part of the reaction, the distance between C1 and N4 is 1.68 Å at **TS2C**, while between C1 and C3 is 1.71 Å at **TS2N**. The C1-C3 and C1-N4 single bond distance was

found to be 1.54 and 1.44 Å at the intermediates **IM1** and **IM2**, respectively. Given that the formation of C-C and C-N single bonds starts at distances of 1.50-1.60 and 1.40-1.60 Å, respectively, these geometrical parameters mean that the formation of C-C and C-N single bonds has not yet started at either of the TSs.

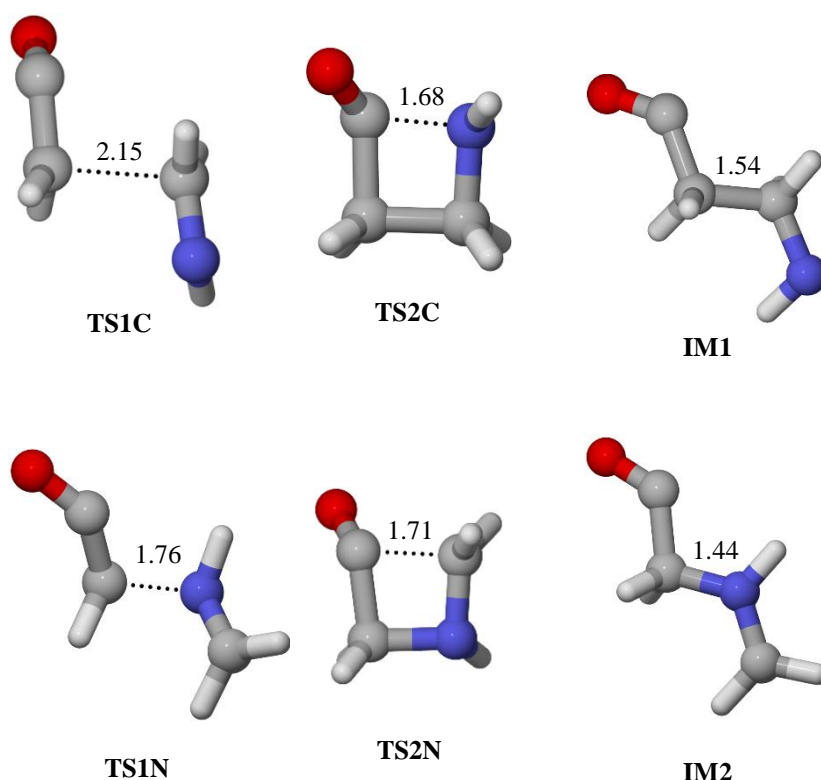


**Figure 3.** B3LYP/6-311++G(d,p) optimised geometries of TSs and intermediates involved in the 22CA reactions of ketene **R1** with methanimine **R2**. Bond lengths are given in Angstroms.

The reactivity in polar cycloaddition reactions can be examined using the global reactivity indices described within the conceptual DFT. The static global properties, namely, global nucleophilicity ( $N$ ), chemical hardness ( $\eta$ ), electronic chemical potential ( $\mu$ ) and global electrophilicity ( $\omega$ ) for the all reactants are listed in Table 3.

The electronic chemical potential ( $\mu$ ) of ketene **R1** is -4.15 eV, which is higher than the **R2** and this indicating that the global electronic flux will be from the **R1** towards the electron-deficient **R2**. The power of electrophilicity for **R1** and **R2** is 1.54 eV and 1.37, which are moderate electrophiles, while **R1** has a nucleophilicity

power of 2.53 eV, which places it in the high nucleophilicity range with in the nucleophilicity

and electrophilicity scale (Domingo, Aurell, Pérez, & Contreras, 2002). However, the power of nucleophilicity for **R2** is 1.87 eV and it falls in the range of moderate nucleophile with in the nucleophilicity and electrophilicity scale (Domingo et al., 2002).

**Table 3.** The chemical hardness ( $\eta$ ), electronic chemical potential ( $\mu$ ), global electrophilicity ( $\omega$ ) and global nucleophilicity ( $N$ ) for all reactants in eV.

Reactant	$\eta$	$\mu$	$\omega$	$N$
<b>R1</b>	5.61	-4.15	1.54	2.53
<b>R2</b>	6.68	-4.27	1.37	1.87

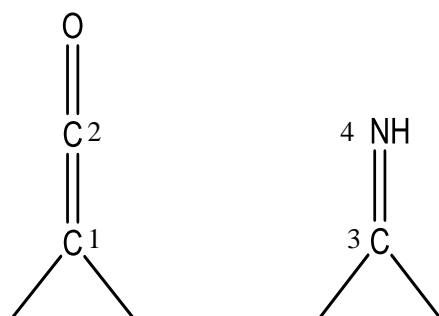


**Figure 4.** Schematic structures and atom numbering of reactants involved in [2+2] cycloaddition reaction.

A good explanation for the study of the regioselectivity in 22CA reactions can be computed by observing at those processes with a pronounced polar character, where the transition structure associated with the rate-determining step mostly involves the formation of one single bond between the most electrophilic and other nucleophilic sites in the 22CA pair of reactants.

**Table 4.** Static Global and Local properties of reactants involved in [2+2] cycloaddition reactions of **R1** and

**R2.**

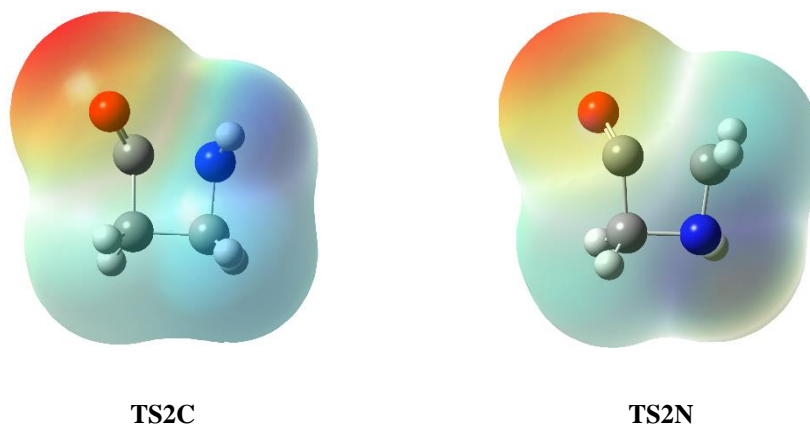
Reactants	site ( $k$ )	$f_k^-$	$f_k^+$
<b>R1</b>	C1	0.54	0.33
	C2	0.06	0.16
<b>R2</b>	C3	0.07	0.91
	N4	0.11	0.18

To represent the charge transfer in a comparable manner, the molecular electrostatic potential (MESP) map of the transition states was obtained. Figure 5 shows the MESP maps for **TS2C** and **TS2N** transition states of two pathways *path1* and *path2*, respectively. The red and blue colors, in the MESP map, indicate the region with higher and lower electron density, respectively. Thus, due to the electrostatic attractive forces between two

interacting fragments, the formation of **TS2C** is more preferable to that of **TS2N**. Table 4 lists the global and local properties of the reactants used in the 22CA reaction of **R1** with **R2**. In reactant **R1**, the nucleophilic site is the C1 carbon (see Figure 4 for atom numbering), which has the highest Fukui function value for an electrophilic attack  $f_k^-$ . Consequently, the most favourable interaction will take place between the C1 center of reactant **R1** and the C3 center of **R2**.

interacting fragments, the formation of **TS2C** is more preferable to that of **TS2N**.

**Figure 5.** The molecular electrostatic potential (MEP) maps of the transition states **TS2C** and **TS2N**.



#### 4. CONSLUSIONS

The B3LYP/6-311++G(d) method was used to study the [2+2] cycloaddition reaction of ketene with methanimine. Two modes of attack between reactants were studied, yielding Azetidin-2-one and Azetidin-3-one as two possible products passing through two different transition states. This reaction are taking place via a stepwise mechanism. It has been noted that, on comparing the energetic results and thermodynamics parameters, the reaction path leading to the formation of Azetidin-2-one are kinetically and thermodynamically more favorable than Azetidin-3-one. The analysis of the frontier molecular HOMO and LUMO orbitals indicates that the Azetidin-2-one (**P1**) are more stable due to its wider energy gab. The global electronic flux from the ketene **R1** to the methanimine **R2** is predicted, because of the high electronic chemical potential and strong nucleophilicity of the ketene **R1** relative to the methanimine **R2**. The analysis of MESP maps for transition states indicates that the formation of **TS2C** is more preferable to that of **TS2N**. The regioselectivity of this cycloaddition is also proposed by electrophilic and nucleophilic Fukui functions.

#### REFERENCES

- Abbiche, K., Mohammad-Salim, H., Salah, M., Mazoir, N., Zeroual, A., El Alaoui El Abdallaoui, H., . . . Hochlaf, M. 2020. Insights into the mechanism and regiochemistry of the 1,3-dipolar cycloaddition reaction between benzaldehyde and diazomethane. *Theoretical Chemistry Accounts*, 139(9), 148. doi: <https://doi.org/10.1007/s00214-020-02662-4>
- Acharjee, N., Mohammad-Salim, H. A., Chakraborty, M., Rao, M. P., & Ganesh, M. 2021. Unveiling the high regioselectivity and stereoselectivity within the synthesis of spirooxindolenitropyrrolidine: A molecular electron density theory perspective. *Journal of Physical Organic Chemistry*, n/a(n/a), e4189. doi:<https://doi.org/10.1002/poc.4189>
- Barber, J. S., Yamano, M. M., Ramirez, M., Darzi, E. R., Knapp, R. R., Liu, F., . . . Garg, N. K. 2018. Diels–Alder cycloadditions of strained azacyclic allenes. *Nature chemistry*, 10(9), 953.
- Ditchfield, R., Hehre, W. J., & Pople, J. A. (1971). Self-Consistent Molecular-Orbital Methods. IX. An Extended Gaussian-Type Basis for Molecular-Orbital Studies of Organic Molecules. *54*(2), 724–728. doi:10.1063/1.1674902
- Domingo, L. R. 2016. Molecular electron density theory: a modern view of reactivity in organic chemistry. *Molecules*, 21(10), 1319.
- Domingo, L. R., Acharjee, N., & Mohammad-Salim, H. A. 2020. Understanding the Reactivity of Trimethylsilyldiazoalkanes Participating in [3+2] Cycloaddition Reactions towards Diethylfumarate with a Molecular Electron Density Theory Perspective. *Organics*, 1(1), 3-18.

- Domingo, L. R., Aurell, M. J., Pérez, P., & Contreras, R. 2002. Quantitative characterization of the global electrophilicity power of common diene/dienophile pairs in Diels–Alder reactions. *Tetrahedron*, 58(22), 4417-4423. doi:[https://doi.org/10.1016/S0040-4020\(02\)00410-6](https://doi.org/10.1016/S0040-4020(02)00410-6)
- Domingo, L. R., Pérez, P., & Sáez, J. A. 2013. Understanding the local reactivity in polar organic reactions through electrophilic and nucleophilic Parr functions. *RSC Advances*, 3(5), 1486-1494. doi:10.1039/C2RA22886F
- Domingo, L. R., Ríos-Gutiérrez, M., & Pérez, P. 2018. A Molecular Electron Density Theory Study of the Reactivity and Selectivities in [3 + 2] Cycloaddition Reactions of C,N-Dialkyl Nitrones with Ethylene Derivatives. *The Journal of Organic Chemistry*, 83(4), 2182-2197. doi:10.1021/acs.joc.7b03093
- Espinosa Ferao, A., & Streubel, R. 2020. 1, 2-Thiaphosphetanes: The Quest for Wittig-Type Ring Cleavage, Rearrangement, and Sulfur Atom Transfer. *Inorganic Chemistry*, 59(5), 3110-3117.
- Flores, D. M., & Schmidt, V. A. 2019. Intermolecular 2 + 2 Carbonyl–Olefin Photocycloadditions Enabled by Cu(I)–Norbornene MLCT. *Journal of the American Chemical Society*, 141(22), 8741-8745. doi:10.1021/jacs.9b03775
- Frisch, M. J., Trucks, G. W., Schlegel, H. B., Scuseria, G. E., Robb, M. A., Cheeseman, J. R., . . . Fox, D. J. 2009. Gaussian 09 B.01. Wallingford, CT.
- Fuentes de Arriba, Á. L., Lenci, E., Sonawane, M., Formery, O., & Dixon, D. J. 2017. Iridium-Catalyzed Reductive Strecker Reaction for Late-Stage Amide and Lactam Cyanation. *Angewandte Chemie International Edition*, 56(13), 3655-3659. doi:10.1002/anie.201612367
- Fukui, K. 1970. Formulation of the reaction coordinate. *The Journal of Physical Chemistry*, 74(23), 4161-4163. doi:10.1021/j100717a029
- Glasnov, T. 2018. Photochemical Synthesis of Heterocycles: Merging Flow Processing and Metal-Catalyzed Visible Light Photoredox Transformations. In *Flow Chemistry for the Synthesis of Heterocycles* (pp. 103-132): Springer.
- Gonzalez, C., & Schlegel, H. B. 1991. Improved algorithms for reaction path following: higher-order implicit algorithms. *The Journal of chemical physics*, 95(8), 5853-5860.
- King, T. A., Stewart, H. L., Mortensen, K. T., North, A. J. P., Sore, H. F., & Spring, D. R. 2019. Cycloaddition Strategies for the Synthesis of Diverse Heterocyclic Spirocycles for Fragment-Based Drug Discovery. *European Journal of Organic Chemistry*, 2019(31-32), 5219-5229. doi:10.1002/ejoc.201900847
- Krylov, A., Windus, T. L., Barnes, T., Marin-Rimoldi, E., Nash, J. A., Pritchard, B., . . . Head-Gordon, T. 2018. Perspective: Computational chemistry software and its advancement as illustrated through three grand challenge cases for molecular science. *The Journal of Chemical Physics*, 149(18), 180901. doi:10.1063/1.5052551
- Kyri, A., Gleim, F., Alcaraz, A. G., Schnakenburg, G., Ferao, A. E., & Streubel, R. 2018. “Low-coordinate” 1, 2-oxaphosphetanes—a new opportunity in coordination and main group chemistry. *Chemical Communications*, 54(52), 7123-7126.
- Kyri, A. W., Gleim, F., Becker, D., Schnakenburg, G., Ferao, A. E., & Streubel, R. 2019. Synthesis of free and ligated 1, 2-thiaphosphetanes—expanding the pool of strained P-ligands. *Chemical Communications*, 55(11), 1615-1618.
- Lee, C., Yang, W., & Parr, R. G. 1988. Development of the Colle-Salvetti correlation-energy formula into a functional of the electron density. *Physical Review B*, 37(2), 785-789. doi:10.1103/PhysRevB.37.785
- Mathew, S., Yella, A., Gao, P., Humphry-Baker, R., Curchod, B. F., Ashari-Astani, N., . . . Grätzel, M. 2014. Dye-sensitized solar cells with 13% efficiency achieved through the molecular engineering of porphyrin sensitizers. *Nature chemistry*, 6(3), 242.
- Mohammad-Salim, H., Hassan, R., Abdallah, H. H., & Oftadeh, M. 2020. The Theoretical Study on the Mechanism of [3+ 2] Cycloaddition Reactions between  $\alpha$ ,  $\beta$ -unsaturated Selenoaldehyde with Nitron and with Nitrile Oxide. *Journal of the Mexican Chemical Society*, 64(2).
- Mohammad-Salim, H. A. 2021. Understanding the Reactivity of C-Cyclopropyl-N-Methylnitron Participating in [3+ 2] Cycloaddition Reactions Towards Styrene with a Molecular Electron Density Theory Perspective. *Journal of the Mexican Chemical Society*, 65(1).
- Mohammad-Salim, H. A., & Abdallah, H. H. 2019a. Theoretical Study for the [2+ 2] Cycloaddition Reaction Mechanism of Ketenes and their Derivatives. *Oriental Journal of Chemistry*, 35(5), 1550-1556.
- Mohammad-Salim, H. A., & Abdallah, H. H. 2019b. Theoretical Study of the [4+ 2] Cycloaddition Reaction of Trifluoroethylene with Five-membered Chalcogens Heterocyclic Compounds. *ARO-THE SCIENTIFIC JOURNAL OF KOYA UNIVERSITY*, 7(2), 69-77.
- Mohammad-Salim, H. A., Abdallah, H. H., Maiyelvaganan, K. R., Prakash, M., & Hochlaf, M. 2020. Mechanistic study of the [2+2] cycloaddition reaction of cyclohexenone and its derivatives with vinyl acetate. *Theoretical Chemistry Accounts*, 139(2), 19. doi:10.1007/s00214-019-2542-y
- Mohammad-Salim, H. A., Acharjee, N., & Abdallah, H. H. 2021. Insights into the mechanism and regioselectivity of the [3 + 2] cycloaddition reactions of cyclic nitron to nitrile functions with a molecular electron density theory perspective. *Theoretical Chemistry Accounts*, 140(1), 1. doi:10.1007/s00214-020-02703-y
- Mohammad-Salim, H. A., Acharjee, N., Domingo, L. R., & Abdallah, H. H. 2020. A molecular electron density theory study for [3 + 2] cycloaddition reactions of

- 1-pyrroline-1-oxide with disubstituted acetylenes leading to bicyclic 4-isoxazolines. *International Journal of Quantum Chemistry*, n/a(n/a), e26503. doi:<https://doi.org/10.1002/qua.26503>
- Mohammad-Salim, H. A., Basheer, H. A., Abdallah, H. H., Zeroual, A., & Jamil, L. A. 2021. A molecular electron density theory study for [3+2] cycloaddition reactions of N-benzylcyclohexylnitron with methyl-3-butenolate. *New Journal of Chemistry*, 45(1), 262-267. doi:10.1039/D0NJ04049E
- Pang, S., Yang, X., Cao, Z.-H., Zhang, Y.-L., Zhao, Y., & Huang, Y.-Y. 2018. Intermolecular [2 + 2] Cycloaddition/Isomerization of Allenyl Imides and Unactivated Imines for the Synthesis of 1-Azadienes Catalyzed by a Ni(ClO<sub>4</sub>)<sub>2</sub>·6H<sub>2</sub>O Lewis Acid. *ACS Catalysis*, 8(6), 5193-5199. doi:10.1021/acscatal.8b01454
- Parr, R. G., & Pearson, R. G. 1983. Absolute hardness: companion parameter to absolute electronegativity. *Journal of the American Chemical Society*, 105(26), 7512-7516. doi:10.1021/ja00364a005
- Parr, R. G., & Weitao, Y. 1989. *Density-Functional Theory of Atoms and Molecules*: Oxford University Press.
- Parr, R. G., & Weitao, Y. 1994. *Density-Functional Theory of Atoms and Molecules*: Oxford University Press.
- Pawlowski, R., Stanek, F., & Stodulski, M. 2019. Recent Advances on Metal-Free, Visible-Light- Induced Catalysis for Assembling Nitrogen- and Oxygen-Based Heterocyclic Scaffolds. *Molecules*, 24(8). doi:10.3390/molecules24081533
- Ríos-Gutiérrez, M., & Domingo, L. R. 2019. Unravelling the Mysteries of the [3+2] Cycloaddition Reactions. *European Journal of Organic Chemistry*, 2019(2-3), 267-282. doi:10.1002/ejoc.201800916
- Saha, R., Chatterjee, A., Mondal, S., Pal, P., Chakrabarty, K., & Das, G. K. 2019. Comparative DFT study on the platinum catalyzed [3+ 2] and [2+ 2] cycloaddition reactions between the derivatives of allene and alkene. *Computational and Theoretical Chemistry*, 1163, 112507.
- Salim, H. A. M., Abdallah, H. H., & Ramasami, P. 2018. *Stereoselectivity and Regioselectivity of the Cycloaddition Dimerization of allyl 3-(2-pyridyl) acrylate and allyl 3-(2-pyrrolyl) acrylate: DFT Calculations*. Paper presented at the IOP Conference Series: Materials Science and Engineering.
- Salim, H. M., Abdallah, H. H., & Ramasami, P. 2018. *Mechanism and Thermodynamic Parameters of Paternò-Büchi Reaction of Benzene and Furan: DFT Study*. Paper presented at the 2018 International Conference on Advanced Science and Engineering (ICOASE).
- Sowmya, D. V., Lakshmi Teja, G., Padmaja, A., Kamala Prasad, V., & Padmavathi, V. 2018. Green approach for the synthesis of thiophenyl pyrazoles and isoxazoles by adopting 1,3-dipolar cycloaddition methodology and their antimicrobial activity. *European Journal of Medicinal Chemistry*, 143, 891-898. doi:<https://doi.org/10.1016/j.ejmech.2017.11.093>
- Svatunek, D., Pemberton, R. P., Mackey, J. L., Liu, P., & Houk, K. 2020. Concerted [4+ 2] and Stepwise (2+ 2) Cycloadditions of Tetrafluoroethylene with Butadiene: DFT and DLPNO-UCCSD (T) Explorations. *The Journal of Organic Chemistry*, 85(5), 3858-3864.
- Tokunova, É. F., Tyurina, L. A., Nikitin, N. A., Nikitina, I. L., Klen, E. É., Khaliullin, F. A., . . . Kantor, E. A. 2001. Quantitative Structure - Activity Relationships for Microsomal Enzymatic System Modulators. Part I: Inhibitors. *Pharmaceutical Chemistry Journal*, 35(6), 322-327. doi:10.1023/A:1012345705162
- Willenbring, D., & Tantillo, D. J. 2008. Mechanistic possibilities for oxetane formation in the biosynthesis of Taxol's D ring. *Russian Journal of General Chemistry*, 78(4), 723-731. doi:10.1134/S1070363208040336
- Xu, C., Zhang, L., & Luo, S. 2014. Merging Aerobic Oxidation and Enamine Catalysis in the Asymmetric  $\alpha$ -Amination of  $\beta$ -Ketocarbons Using N-Hydroxycarbamates as Nitrogen Sources. *Angewandte Chemie International Edition*, 53(16), 4149-4153. doi:10.1002/anie.201400776